

Optimized oxygen deprived low temperature sputtered WO₃ thin films for crystalline structures

Sidra Farid¹, Bo Hsu¹, Liliana Stan², Michael Stroschio^{1,3,4}, Mitra Dutta^{1,3}

¹Department of Electrical and Computer Engineering, University of Illinois at Chicago, Chicago, Illinois 60607, USA

²Center for Nanoscale Materials, Argonne National Labs, Lemont, Illinois 60493, USA

³Department of Physics, University of Illinois at Chicago, Chicago, Illinois 60607, USA

⁴Department of Bioengineering, University of Illinois at Chicago, Chicago, Illinois 60607, USA

Abstract

We report a detailed analysis on the effects of processing parameters for sputtered tungsten tri oxide (WO₃) thin films on their structural, vibrational and electrical properties. The research aims to understand fundamental aspects of WO₃ sputtering at relatively lower temperatures and oxygen deprived environment targeting applications of temperature and oxygen sensitive substrates. Structural analysis indicates that films deposited at room temperature or substrate temperatures at or below 400°C with low oxygen partial pressure are amorphous. Crystallization of the films were observed with distinct Raman peaks when the films were annealed at 300°C or above using rapid thermal annealing for 10 minutes. Films revealed monoclinic phases of WO₃ with the presence of W-O-W stretching, bending and lattice vibrational modes in the Raman spectra. Interestingly, change of transport behavior from insulating to semiconducting were observed for as deposited films on post annealing. Annealed films revealed stoichiometric WO₃ phases with no external defects detected. The present study adopts a route to intercalate WO₃ in variety of applications from electrochromic coloration to a crystalline thin film for electronic devices sensitive to higher temperatures and gas flow in the sputtering system.

Introduction

Tungsten oxide films have been extensively studied for their outstanding electrochromic properties due to its numerous potential applications in smart windows [1], gas sensors [2] and photo catalysts [3]. It has been reported that WO₃ films exhibit high coloration efficiency, excellent cyclic stability and faster Li⁺ insertion than many other metal oxides [4]. The area that has not been explored in detail is the use of nanoscale WO_x as an active layer for extraordinary potential in future energy-related applications. Recent studies have also shown that sulfurization and salinization of WO₃ thin films are promising for large area growth of two dimensional WS₂ and WSe₂ nanosheets [5]. The next generation of outperforming electronic devices will be led by materials offering robust solutions for sustainability and efficiency of the devices. For example, WO₃ being a high electron affinity oxide (EAO) can be integrated with p-type hydrogen terminated diamond for the development of high frequency high power field effect transistors (FETs). Torjman *et al.* [6] has reported WO₃ and ReO₃ as an efficient surface charge transfer dopant for high band gap materials whereas Yin *et al.* [7] has recently demonstrated first diamond/H terminated FET with WO₃ as a surface electron acceptor materials.

With WO_3 , MoO_3 and Nb_2O_5 emerging strongly as a good candidate for surface charge transfer oxide materials other than their electrochromic applications, low mobility and deteriorated film quality are essential issues affecting the ultimate performance of fabricated devices [8]. These issues have not been dealt with in detail in the past and a fundamental understanding on the film quality, structural behavior and vibrational modes associated with the deposited structure remains a huge challenge. It is noted that studies on electrochromic properties of WO_3 devices and their electrical performance have been reported previously but to our knowledge, no detailed report on correlation between vibrational states of WO_3 films and film quality is reported discussing the effects of process conditions on deposited films.

In most WO_3 applications, WO_3 thin films have been deposited using sol-gel technique, oxidation of elemental tungsten films, physical vapor deposition and magnetron sputtering [9]. Among the various deposition techniques, radio frequency (RF) magnetron sputtering offers added advantage of relatively affordable and scalable deposition method, uniform film quality and the flexibility to optimize deposition conditions as per need. Despite these facts, previous studies on sputtered WO_3 thin films were not being optimized based on applications towards surface charge transfer. The challenge with this deposition technique that researchers encounter is sensitivity of the substrates that could be affected by high insertion of oxygen content, high deposition temperatures and plasma exposure associated with sputtering process [10]. Infact most of the preparation methods utilized so far include higher than 600°C to enhance the crystallinity of the amorphous WO_3 films which ultimately limits the scope of possible applications. Herein we have utilized a systematic step by step approach that endeavors to crystalline stoichiometric films in oxygen deprived environment and relatively low temperatures.

It is well known that annealing is one of the most effective ways to influence the structure and film quality [11]. Low temperature annealing is one simple solution that's leads to long term durability of the compounds by eliminating defects and improving structural homogeneity. We have utilized post deposition treatment of rapid thermal annealing (RTA) for short duration of time to crystallize films that are sensitive to longer heat treatments. By varying the processing parameters during deposition and post annealing at different temperatures, a route to modify electrical, structural and vibrational states of the deposited films is established. The knowledge obtained by this study can be useful to address issues with stability and degradation of various devices including electrochromic devices.

Experimental

(i) *Film Deposition:*

Tungsten tri-oxide films used in this study were prepared by reactive RF sputtering on a Si/SiO₂ substrates with a tungsten trioxide target (99.9%, Kurt J. Lesker Co., 2 inch diameter) in a controlled argon/oxygen ambient. The base pressure of the deposition chamber (AJA International) was below $2 * 10^{-7}$ Torr. The pressure during deposition was maintained at 5 or 8 mTorr while the $\text{O}_2/(\text{O}_2+\text{Ar})$ flow ratio was changed from 0 to 7%. RF power was kept constant at 100 W. The Si/SiO₂ wafers were cleaned in an acetone/isopropanol/deionized water rinse prior to deposition.

Characterizations of the film included profilometry (Veeco, Dektak 8), Raman Spectroscopy, X-ray diffraction (XRD), X ray photoelectron spectroscopy (XPS), energy dispersive X-ray (EDX) analysis and resistivity measurements. Film thickness was measured by contact Profilometer (Dektak 8).

(ii) Characterization

The Raman spectra was taken in the back scattering geometry using a Reinshaw Raman inVia confocal microscope system with 514 nm non-resonant excitation wavelength of an argon-ion laser. The grating used was 1800 grooves/mm providing 2 cm^{-1} resolution. All experiments were repeated over multiple samples for reproducibility.

The crystallinity of the films was investigated by X-Ray diffraction (XRD). The stoichiometry was analyzed by x-ray photoelectron spectroscopy (XPS) using Kratos AXIS-165 spectrometer with a monochromatic AlK α X-ray source (1486.6 eV) and a multichannel detector. Spectra was obtained using both survey mode (pass energy of 80 eV) and high-resolution mode for C 1s, O 1s and W 4f (pass energy of 20 eV). Binding energies for the high-resolution spectra were calibrated by setting C 1s at 284.6 eV. The elemental composition was assessed using energy dispersive Xray (EDX) spectroscopy attached with the variable-pressure Hitachi S-3000N scanning electron microscope. Electrical measurements were done using two and four probe measurement setup in a home-built probe station with Kethley 2400 source meter.

Rapid thermal annealing (RTA) was done in an annealing chamber for 10 minutes at 400°C and 500°C. A typical annealing run consisted of annealing in for 10 min at a rate of 60 °C/sec to 400°C and holding for 1 min before actual anneal duration, followed by rapid cooling.

Results and Discussions

WO₃ thin films were sputtered on Si/SiO₂ substrates under various conditions as shown in Table 1. Sample #1 was grown with O₂ starved condition for 1 hr in the presence of only Ar gas at a pressure of 5 mTorr. Sample # 2 and 3 utilized 5 mTorr pressure in Ar and O₂ deprived environment keeping O₂/(O₂+Ar) ratio being 7%. The deposition rate for sample 2 and 3 was 0.78 and 0.75 Å/s respectively. By visual inspection of WO₃ being an electrochromic material, the sputtered films (samples # 1-3) span the range from sub stoichiometric WO_{3-x} (metallic grey/blue color) to fully oxidized WO₃ films (sample #4-6) (yellow/green color) as confirmed in literature studies [5] [8] (Supplementary Figure 1). It is also observed that the deposition rate decreases as deposition pressure increases.

Table 1:
Tungsten oxide films on Si/SiO₂, produced at different oxygen-argon gas flows and pressures

Sample	Deposition Pressure (mTorr)	O ₂ Flow Rate (sccm)	Ar Flow Rate (sccm)	Deposition Rate (Å/s)	Deposition Temperature (°C)
1	5	0	26	0.7	RT
2	5	2	26	0.78	RT
3	5	2	26	0.75	RT
4	8	2	26	0.63	RT
5	8	2	26	0.66	RT
6	8	2	26	0.66	300
7	8	2	26	0.66	400

Raman spectra for as deposited WO₃ samples (sample# 1- 4) are shown in Figure 1. The visible sharp peak at 520.7 cm⁻¹ for all the samples originates from well-known strong Si Raman peak [12]. Sample #1 (metallic grey visual color) with no oxygen content demonstrates distinct peak

characteristics at 808, 712, 268 and 134 cm^{-1} . Thicker film in sample #1 reveal clear WO_3 Raman signatures as compared to picking the interface modes or enhanced sub Si Raman lines. The dominant higher order bands at 808 and 712 cm^{-1} represents the W–O–W stretching modes while the smaller peaks at 268 and 134 cm^{-1} corresponds to the O–W–O bending modes [13]. Studies have revealed secondary peaks next to the primary stretching modes on fitting with Lorentzian line shapes [14]. As a comparison, a thicker WO_3 commercial powder was taken that reveals similar data under Raman spectroscopy (Supplementary Fig. 2)

On adding low rate oxygen pressure (sample #2, 3 and 4), Raman spectra shows broad bands in two regions, 650 – 850 cm^{-1} and 200 – 350 cm^{-1} . A clear hump at $\sim 808 \text{ cm}^{-1}$ shows signature of WO_3 films while a large variety of bond lengths or disordered structures could be responsible for the broad Raman bands of the films [13]. Although lower pressure can give a highly dense film with good crystallinity, we increased the pressure of sample #4 to 8 mTorr in order to ensure if the bombarded electrons in the sputtering system has less effect on the substrate. This might not be a critical step for Si substrates or devices insensitive to deposition technique but play a key role in substrates where the system could be impacted by sputtering pressure and plasma conditions such as H-terminated diamond substrates. Bending mode of WO_3 at 272 cm^{-1} was also seen for this sample along with other modes. As a calibration substrate, Raman data was taken on bare Si/ SiO_2 sample with no WO_3 film on it (reference sample). The sample shows flat response in the expected broad range spectra of WO_3 650 – 850 cm^{-1} . The well-known Si peaks are revealed as described in detail in Table 2 for all the samples.

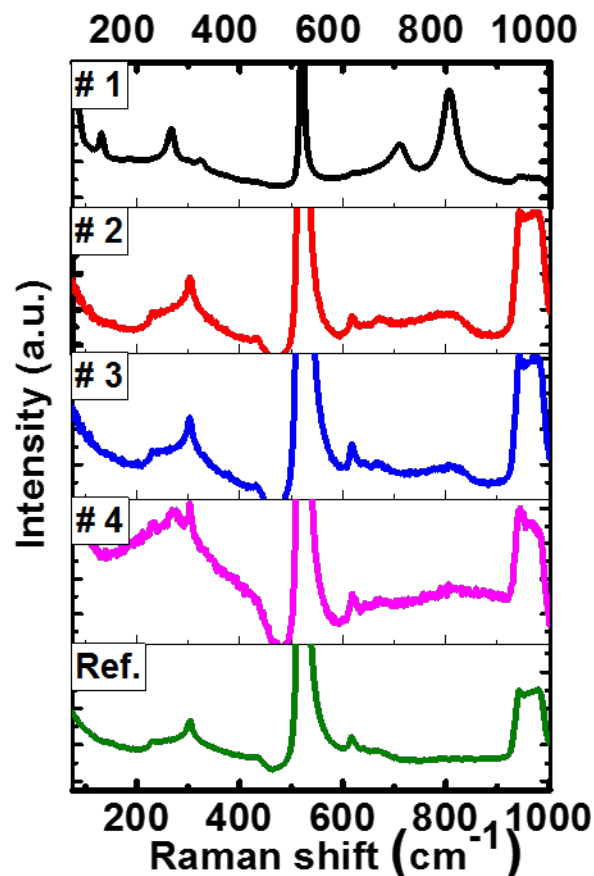


Figure 1: Raman spectra using 514 nm excitation laser for samples #1-4 with exposure time of 10s ; Reference sample of bare Si/ SiO_2 taken for calibration

Table 2:

Raman peaks and resistance measurements of Tungsten oxide films (sample #1-4) on Si/SiO₂, produced at different Oxygen-Argon gas flows and pressures; Ref. is a calibration sample with bare Si/SiO₂ wafer

Sample #	Raman Peaks (cm ⁻¹)									Resistance
	a	b	c	d	e	f	g	h	i	
1	134	-	268	-	520.7	-	712	808	960	Semiconducting
2	-	234	-	303	520.7	620	-	806	961	Insulating
3	-	231	-	303	520	619	-	808	961	Insulating
4	-	233	275	304	520.1	617	-	808.1	959	Insulating
Ref.	-	228	-	303	520.7	618	-	-	964	N/A

In order to explore more on the electrical properties of the films, resistance measurements are taken using two-probe measurement setup. Typically, semiconducting films have two-terminal resistance across the entire substrate (~1 cm²) of ~ 100 MΩ, while insulating films have two-terminal resistance > 5GΩ. The films deposited at room temperature without oxygen were less resistive as compared to films underwent Ar/O₂ atmosphere that were insulating (Table 2). Resistivity measurement is a critical factor in order to find stable and efficient surface acceptor materials. Less resistive oxide layer may act as a shunt resistor and lead to reduced performance of diamond FETs. Change of conductivity on either heating, gas flow variations or applying voltage is a turning factor for choosing EAO [15]. Thus standalone vibrational states for a material with clear surface phonon modes could be misleading for practical electronic device processing and their reliability. X-ray diffraction (XRD) measurements in 2-theta geometry were also performed on the WO₃ films to study the crystal structure. All the films appear to be amorphous and does not exhibit diffraction peaks as presented in Figure 2.

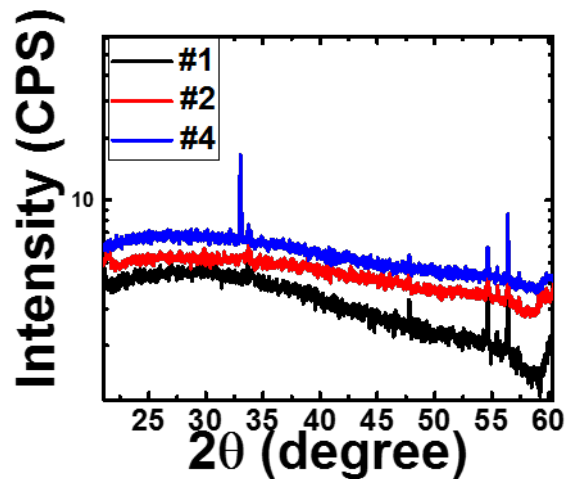


Figure 2: XRD patterns for Sample #1 (lowest plot), Sample #2 (middle plot) and Sample #4 (top curve) showing amorphous WO₃ films

Further samples deposited at room temperature with optimized thickness of 20 nm vs deposition temperature at 300°C and 400°C were demonstrated. Lower temperatures were chosen to avoid surface termination damage on substrates sensitive to much higher temperatures. All the deposited films are found to be insulating. The deposited WO₃ films still

reveals amorphous nature of the films and did not show a sign of crystallinity. Raman data does indicate signs of WO_3 films at $\sim 803 \text{ cm}^{-1}$ and $\sim 300 \text{ cm}^{-1}$ (shown by rectangles in Figure 3) but there are no visible peaks emerging from these films. We confirmed presence of tungsten, oxygen, carbon and silicon with EDX data (Supplementary Fig. 3).

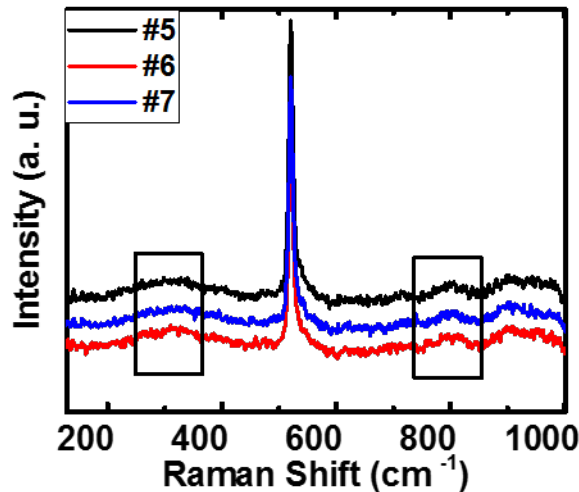


Figure 3: Raman spectra of as-deposited WO_3 at room temperature (Sample#5), 300°C (Sample#6), and 400°C (Sample#7) under 514 nm excitation laser; two rectangles indicates signature of WO_3 films

Samples #5 ,6 & 7 underwent rapid thermal annealing treatments (RTA) for 10 minutes under vacuum. RTA has been demonstrated as an important way to improve the crystal quality of various films such as GaAs, GaInNAs quantum wells or formation of ohmic contacts [16]. RTA was chosen in our study over conventional annealing techniques due to the fact that our study revolves around dealing with substrates sensitive to high temperature deposition or annealing. Also RTA has proven to generate results with both reproducibility and repeatability.

Raman spectra was taken after samples went annealing treatments as shown in Figure 4. All the samples show distinct WO_3 peaks around 300 cm^{-1} and 800 cm^{-1} that were hidden or showing broad spectrum before undergoing thermal treatment. The dominant peaks around 696 cm^{-1} and 806 cm^{-1} represent the O–W–O stretching modes and the smaller peaks around 300 cm^{-1} correspond to the O–W–O bending vibrational modes [13]. There is another Raman peak that originates at 696 cm^{-1} only for annealed samples. The fact that after a thermal treatment at 400 and 500°C , the film structures tend to be more stable as compared to before while W–O–W bond could become shorter. This results in formation of new bond that is depressed as compared to strong 807 cm^{-1} symmetric stretching vibrational mode [17]. Peak 131 cm^{-1} doesn't seem to be a characteristic of WO_3 and thought to originate from any surface adsorbents or from the system itself. Other Raman peaks that are originating from Si substrate are mentioned in earlier discussion.

The Raman bands of WO_3 are shifted towards lower and higher wavenumbers in different regions after heat treatment as presented in detail in Table 3. Nevertheless, shifts of Raman peaks often happen because of the differences in morphologies, sizes and crystal phases of tungsten trioxide films. Thummavichai *et al.* has presented a detailed study on change in lattice spacing of WO_3 nanoparticles that was affected by the heat treatment [13]. Disordered structure or various bond lengths are considered responsible for the broad Raman peaks seen for

unannealed films. Meanwhile it is believed that relatively larger number of oxygen vacancies are a key factor in observing broad Raman peaks as observed for unannealed or as-deposited samples. As the films are annealed, crystallization and oxidation of deposited tungsten trioxide films resulted in several distinct Raman peaks in the spectrum. This is due to the formation of stable W-O bonds that will be confirmed in our XRD study.

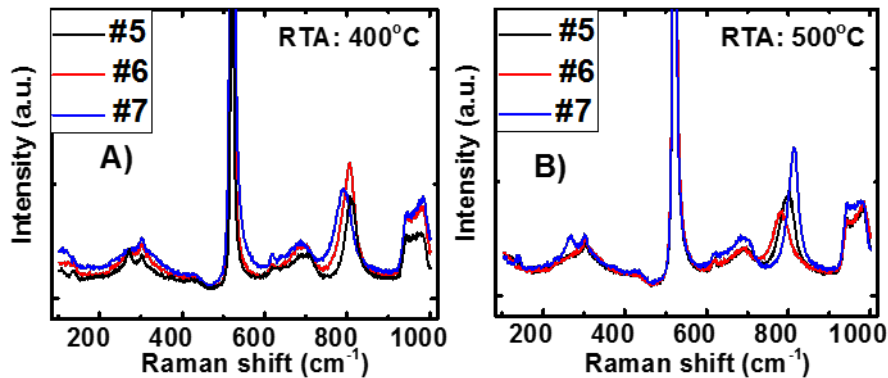


Figure 5: XRD patterns of a) as-deposited film (sample #5) and annealed at 400 and 500 °C;

Another interesting observation was revealed on electrical characterization of all these films. Annealed films that were deposited at room temperature showed change in resistivity and became semiconducting from insulating films (Table 3). Samples annealed at 500 °C also showed lower resistance compared to samples annealed at 400 °C. Similar results have been revealed by Jingze Li who reported that conductivity of WO₃ is abruptly promoted on annealing treatment whereas have negligible impact on optical transmittance in visible spectrum region [18].

Table 3:

Rapid thermal annealing on Tungsten trioxide films produced at room temperature (sample#5), 300°C (sample#6) and 400°C (sample#7) at annealing temperatures of 400°C and 500°C for 10 minutes in air ambient

Sample#	RTA Anneal: 400°C									
	Resistance	Structure	WO ₃ Raman peaks (cm ⁻¹)							
5	4 MΩ	Monoclinic	137	271	304	520	617	696	807	961
6	200 MΩ	Monoclinic	137	-	302	520.1	623	696	806	961
7	420 MΩ	Monoclinic	-	-	304	520	618	687	788	961
Sample#	RTA Anneal: 500°C									
	Resistance	Structure	WO ₃ Raman peaks (cm ⁻¹)							
5	2 MΩ	Monoclinic	-	-	302	520	621	694	802	960
6	54 MΩ	Monoclinic	-	-	301	520.1	621	694	784	961
7	270 MΩ	Monoclinic	137	265	301	520	621	685	814	961

Although conversion of transport behavior from highly insulating to semi-insulating took place with annealing treatment for as deposited WO₃ films, structural evolution of WO₃ films from amorphous to crystalline is also revealed as shown in Figure 5.

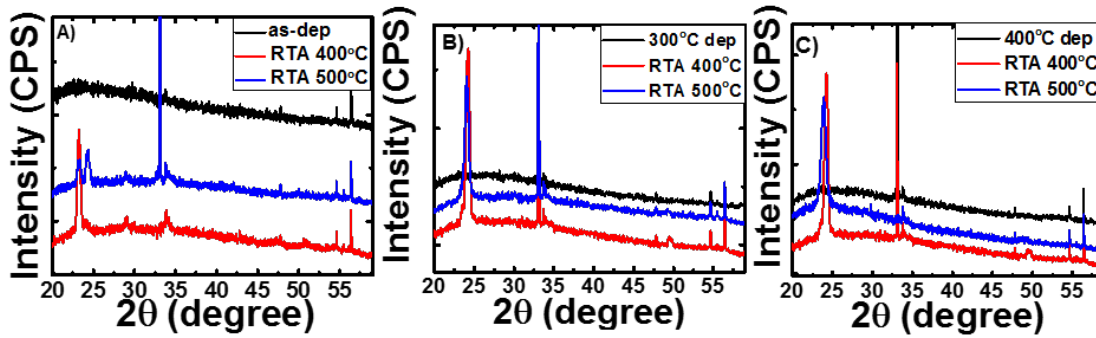


Figure 5: XRD patterns of a) as-deposited film (sample #5) and annealed at 400 and 500 °C; b) WO₃ film deposited at 300°C (sample #6) and annealed at 400 and 500 °C; c) WO₃ film deposited at 400°C (sample #7) and annealed at 400 and 500 °C

It is revealed that all annealed films show sharp diffraction peaks indicating crystallization of the films irrespective of whether the films were as-deposited or deposited at higher temperatures. A distinct monoclinic (002) peak at $2(\theta) = 23.16^\circ$ are clear traces of all samples annealed at 400°C and 500°C. Peak appearing at 24.07° and 24.2° for as deposited sample annealed at 500 °C are assigned to (020) and (200) planes of the monoclinic WO₃ films [17]. It is noticed that intensities distribution of peaks vary between the samples whereas room temperature deposited samples have relatively lower intensities. This could possibly arise from preferred crystal orientation or from the presence of crystallographic shear planes as also explained by Feng et al. [19]. It is also concluded that crystallization occurs even at 400°C post annealing therefore higher temperature annealing is not required. Thus, the process indicates a complete transformation from amorphous to crystalline films as confirmed by XRD data.

Further we analyzed WO₃ thin films by XPS data for few samples to obtain precise results on their chemical composition. Figure 6 (a) and (c) shows a typical survey spectrum of sample #5, 6 & 7 of WO₃ films annealed at 400°C. Apart from the weak C 1s peak position in both samples, which is attributed to adsorbed species on the film surface, no spurious peaks from foreign ions are detected and only tungsten and oxygen related core levels are seen. Apart from wide scan spectra, high resolution scan of W 4f and O 1s spectra for few samples are recorded. It is known that W and O peaks shifts depending on W and O stoichiometry. Observed W 4f region comprised of a single doublet for all samples investigated with binding energies of 35.8 for W 4f_{7/2} and 37.8 eV for W 4f_{5/2}. This is a close agreement with the WO₃ energies reported in literature [5] [20]. Position of the peaks and symmetry of tungsten line shapes can be resonated with the fact that tungsten was close to 100% present in its W^{VI} oxidation state. These results are also confirmed by finding peak position of O 1s peak which is a close match of oxygen in WO₃ [20]. Thus quantitative analysis of O-W ratio reveals that WO₃ is found closed to its stoichiometric formulation within the estimated error bar.

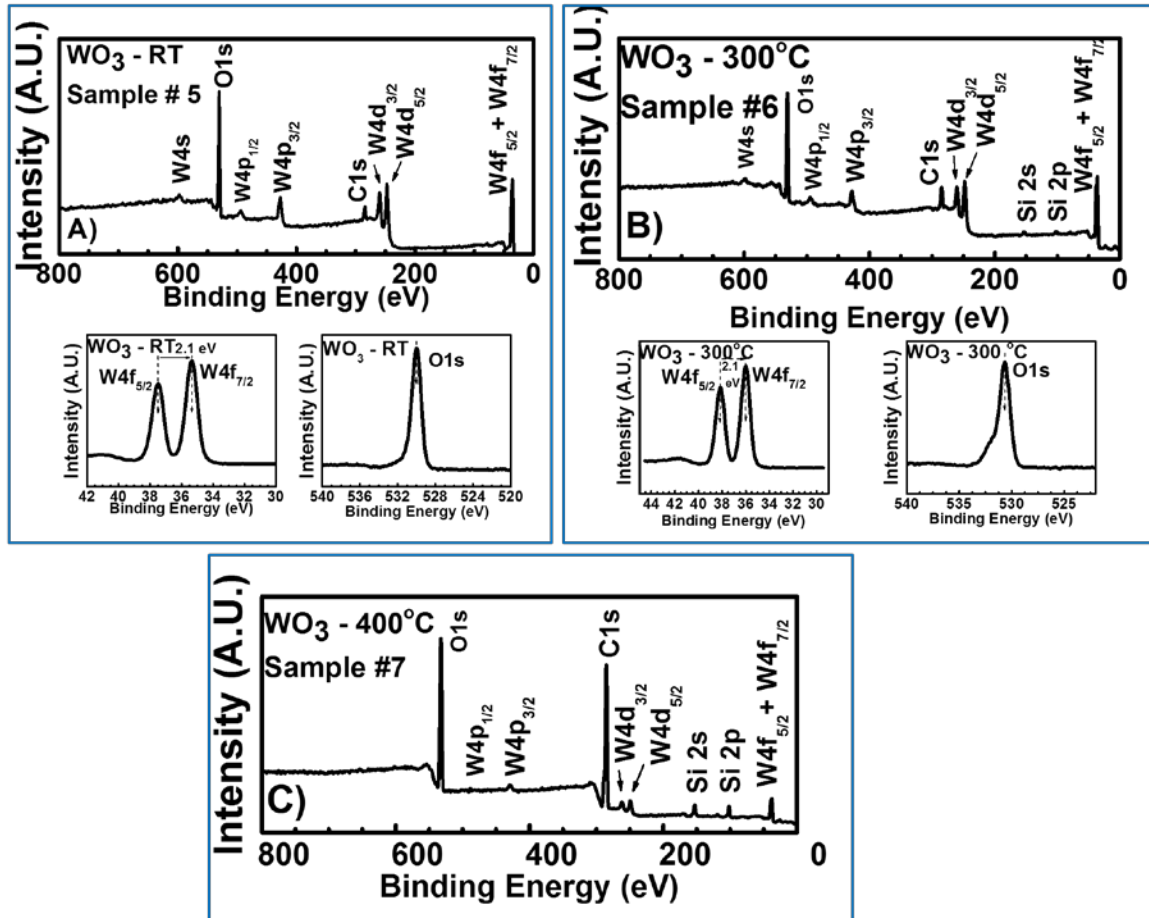


Figure 6: XPS survey scan of the A) as-deposited (sample # 5); B) 300°C deposited WO_3 films (Sample# 6) and C) 400°C deposited WO_3 films (Sample# 7); all annealed at 400 °C after RTA ; Sample # 5 and 6 also indicate high resolution scan of W 4f and O 1s respectively

Conclusions

In conclusion, WO_3 thin films have been grown using RF magnetron sputtering. Characterization reveals high-quality WO_3 films after RTA process. Effects of relatively lower annealing temperatures on the structure and optical properties reveal that WO_3 crystallizes into monoclinic phase for post annealing treatments at 300°C or above. Results from Raman spectra further confirms crystallinity with distinct vibrational peaks of W-O bonds after post annealing. Stoichiometric WO_3 phases in the films are produced as revealed from XPS data presented. Electrical response of the films shows transition of transport behavior from highly insulating to semi-insulating with annealing treatment for as deposited WO_3 films. The present data could therefore significantly help developing strategies to use WO_3 as an active layer for devices sensitive to higher temperatures and reduced oxygen flow in the sputtering system.

Acknowledgments

This work was supported by Collaborative Agreement No. W911NF1920086 from the Army Research Labs, USA. This work made use of instruments in the Electron Microscopy Service and Raman spectroscopy in Research Resources Center, UIC. Use of the Center for Nanoscale Materials, an Office of Science user facility, was supported by the US Department of Energy,

References

- [1] Svensson, J. S. E. M., and C. G. Granqvist. "Electrochromic coatings for smart windows: crystalline and amorphous WO₃ films." *Thin Solid Films* 126, no. 1-2 (1985): 31-36.
- [2] Li, Xiao-Lin, Tian-Jun Lou, Xiao-Ming Sun, and Ya-Dong Li. "Highly sensitive WO₃ hollow-sphere gas sensors." *Inorganic chemistry* 43, no. 17 (2004): 5442-5449.
- [3] Chen, Di, and Jinhua Ye. "Hierarchical WO₃ hollow shells: dendrite, sphere, dumbbell, and their photocatalytic properties." *Advanced Functional Materials* 18, no. 13 (2008): 1922-1928.
- [4] Ozer, N., and C. M. Lampert. "Electrochromic performance of sol-gel deposited WO₃-V₂O₅ films." *Thin Solid Films* 349, no. 1-2 (1999): 205-211.
- [5] Salitra, G., G. Hodes, E. Klein, and R. Tenne. "Highly oriented WSe₂ thin films prepared by selenization of evaporated WO₃." *Thin solid films* 245, no. 1-2 (1994): 180-185.
- [6] Tordjman, Moshe, Kamira Weinfeld, and Rafi Kalish. "Boosting surface charge-transfer doping efficiency and robustness of diamond with WO₃ and ReO₃." *Applied Physics Letters* 111, no. 11 (2017): 111601.
- [7] Yin, Zongyou, Moshe Tordjman, Alon Vardi, Rafi Kalish, and Jesús A. del Alamo. "A diamond: H/WO₃ metal-oxide-semiconductor field-effect transistor." *IEEE Electron Device Letters* 39, no. 4 (2018): 540-543.
- [8] Aegerter, Michel A., Cesar O. Avellaneda, Agnieszka Pawlicka, and Mohamed Atik. "Electrochromism in materials prepared by the sol-gel process." *Journal of Sol-Gel Science and Technology* 8, no. 1-3 (1997): 689-696.
- [9] Buch, V. R., Chawla, A. K., & Rawal, S. K. (2016). Review on electrochromic property for WO₃ thin films using different deposition techniques. *Materials Today: Proceedings*, 3(6), 1429-1437.
- [10] Deb, Satyen K. "Opportunities and challenges in science and technology of WO₃ for electrochromic and related applications." *Solar Energy Materials and Solar Cells* 92, no. 2 (2008): 245-258.
- [11] Farid, Sidra, Michael A. Stroschio, and Mitra Dutta. "Multiphonon Raman scattering and photoluminescence studies of CdS nanocrystals grown by thermal evaporation." *Superlattices and Microstructures* 115 (2018): 204-209.
- [12] Parker Jr, J. H., D. W. Feldman, and M. Ashkin. "Raman scattering by silicon and germanium." *Physical Review* 155, no. 3 (1967): 712.
- [13] Thummavichai, Kunyapat, Liam Trimby, Nannan Wang, C. David Wright, Yongde Xia, and Yanqiu Zhu. "Low temperature annealing improves the electrochromic and degradation behavior of tungsten oxide (WO_x) thin films." *The Journal of Physical Chemistry C* 121, no. 37 (2017): 20498-20506.
- [14] Meenakshi, M., R. Sivakumar, P. Perumal, and C. Sanjeeviraja. "Studies on electrochromic properties of RF sputtered Vanadium Oxide: Tungsten Oxide thin films." *Materials Today: Proceedings* 3 (2016): S30-S39.
- [15] Gillet, M., K. Aguir, C. Lemire, E. Gillet, and K. Schierbaum. "The structure and electrical conductivity of vacuum-annealed WO₃ thin films." *Thin Solid Films* 467, no. 1-2 (2004): 239-246.
- [16] Lee, Byoung Hun, Laegu Kang, Renee Nieh, Wen-Jie Qi, and Jack C. Lee. "Thermal stability and electrical characteristics of ultrathin hafnium oxide gate dielectric reoxidized with rapid thermal annealing." *Applied Physics Letters* 76, no. 14 (2000): 1926-1928.
- [17] Marsen, Bjorn, Brian Cole, and Eric L. Miller. "Influence of sputter oxygen partial pressure on photoelectrochemical performance of tungsten oxide films." *Solar Energy Materials and Solar Cells* 91, no. 20 (2007): 1954-1958.
- [18] Li, Jingze, Masayuki Yahiro, Kenji Ishida, Hirofumi Yamada, and Kazumi Matsushige. "Enhanced performance of organic light emitting device by insertion of conducting/insulating WO₃ anodic buffer layer." *Synthetic Metals* 151, no. 2 (2005): 141-146.
- [19] Feng, Zhang, Wang Hai-Qian, Wang Song, Wang Jing-Yang, Zhong Zhi-Cheng, and Jin Ye. "Structures and optical properties of tungsten oxide thin films deposited by magnetron sputtering of WO₃ bulk: Effects of annealing temperatures." *Chinese Physics B* 23, no. 9 (2014): 098105.
- [20] Cantalini, Carlo, H. T. Sun, Marco Faccio, M. Pelino, S. Santucci, Luca Lozzi, and Maurizio Passacantando. "NO₂ sensitivity of WO₃ thin film obtained by high vacuum thermal evaporation." *Sensors and Actuators B: Chemical* 31, no. 1-2 (1996): 81-87.

Supplementary Data

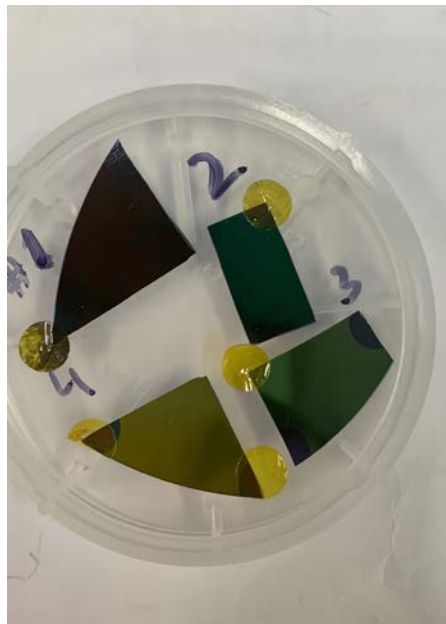


Figure 1: Samples # 1-4 revealing metallic grey, blue, green and yellow color as per stoichiometric ratios

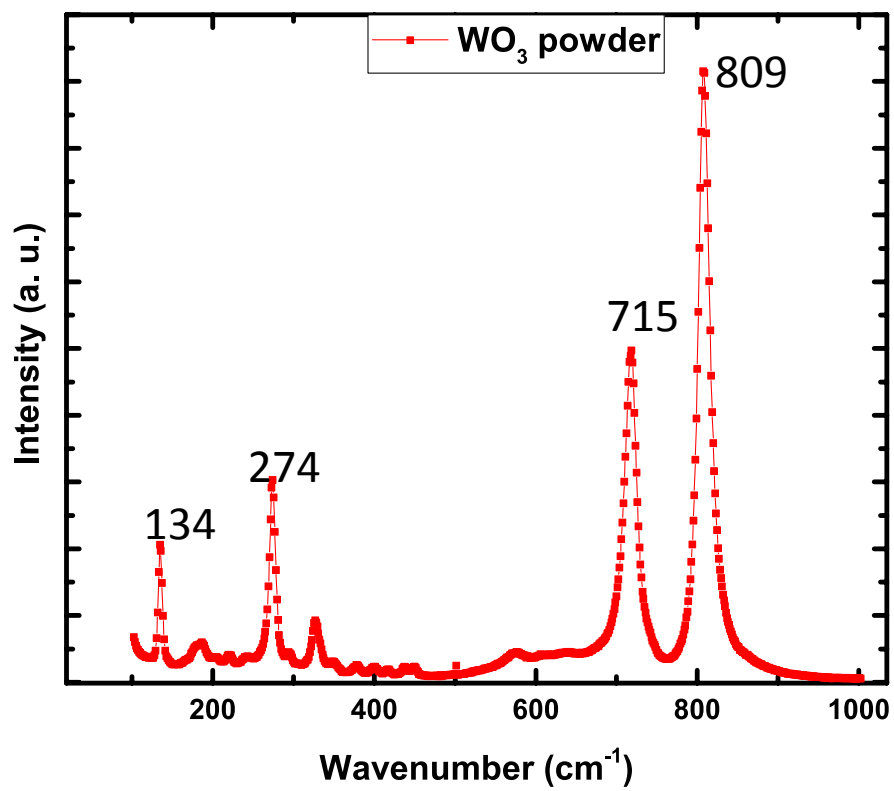


Figure 2: Raman spectra of WO₃ powder

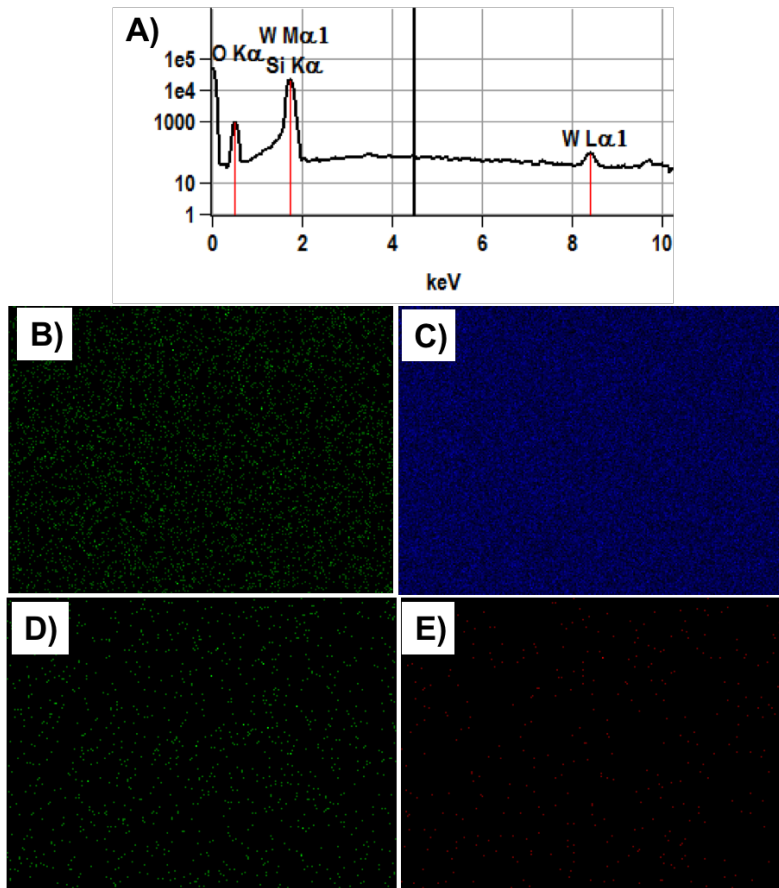


Figure 3: EDX profile for WO_3 film; (B) Mapping of data showing oxygen content; (C) mapping data for Si; (D) mapping data for tungsten content; (E) mapping data for carbon adsorbents